

Supercritical fluid-micronized ipratropium bromide for pulmonary drug delivery

Yong Ho Kim, Katherine S. Shing *

Mork Family Department of Chemical Engineering and Materials Science, University of Southern California, Los Angeles, CA 90089-1211, USA

Received 19 October 2006; received in revised form 10 April 2007; accepted 24 April 2007

Available online 1 May 2007

Abstract

Ipratropium bromide (IB) was micronized by means of a CO₂-based aerosol solvent extraction system (ASES) in order to improve the particle shape and size characteristics for use in inhalation therapy. The particle size parameter most relevant to pulmonary delivery is the aerodynamic diameter. In this study, ASES experiments were conducted using various liquid solvents for IB such as dimethylformamide (DMF), ethanol (EtOH), and mixtures of ethanol and acetone (EtOH/Ac). Several operating parameters were varied including temperature, pressure, IB concentration in the liquid solution, and the solution injection rate. The particles were analyzed by scanning electron microscopy (SEM). The true density of the particles was measured using a pycnometer and the mass median aerodynamic diameter (MMAD) determined. The results indicate that the size and morphology of the microparticles are most sensitive to solvent choice. Optimum results were obtained when IB particles were precipitated from DMF. The particles were more regular in shape, slightly elliptical, not agglomerated, and within the aerodynamic diameter range of 0.6–3.0 μm . Fourier transform infrared (FTIR) studies indicate no structural deformation as result of the ASES process. The regional depositions of inhaled IB particles were estimated using a multiple-path model of particle deposition (MPPD). The results indicate that IB particles with MMAD in the range of 2–3 μm deposited mainly in the respiratory airways in the lung.

© 2007 Published by Elsevier B.V.

Keywords: Ipratropium bromide; Supercritical antisolvent; Aerosol solvent extraction system; Pulmonary delivery; Aerodynamic diameter

1. Introduction

Pulmonary drug delivery technology has undergone significant advancement over the last 20 years. Pulmonary route of administration offers a number of advantages over other administrations such as oral and parenteral routes of drug delivery, including the use of lower dose than by the oral route to achieve the same therapeutic benefit, degradation within the gastrointestinal tract is avoided, a reduction of unwanted systemic side effects, and a more rapid onset of action. One of the major prerequisites for a successful pulmonary drug application is suitable particle size. In general, it is widely accepted that particles with aerodynamic diameter of 1 to 5 μm are most likely to deposit in the lung, but only those in the 2 ~

3 μm size range are involved in peripheral/deep lung (alveolar) deposition [1,2]. Deposition characteristics of a respirable particle depend primarily on its aerodynamic diameter, which is a function of particle size, shape and density [3]. Particles larger than 10 μm are deposited in the upper respiratory tract, e.g., the mouth, larynx and trachea, whereas particles between 0.1 and 0.5 μm are exhaled from the lungs without depositing [4].

Conventional micronization processes [5–7] such as jet milling and spray drying can result in wide size distribution, thermal denaturing, excessive surface change or roughness and hence limit good control of the particle material characteristics. Supercritical fluid (SCF) technology has been shown to be an effective route for particle formation for pulmonary drug delivery. It avoids most of the drawbacks of the conventional micronization techniques, and offers the advantages of solvent-free product, control of crystal polymorphism, mild operating temperature, single-step process, and being environmentally benign [8–13].

* Corresponding author. Tel.: +1 213 740 2068; fax: +1 213 740 8053.

E-mail address: shing@usc.edu (K.S. Shing).

In the past 15 years, SCF technology has been employed to micronize a number of pharmaceutical compounds for pulmonary delivery including erythromycin [14], sodium cromoglycate [15], salbutamol [16], salmeterol xinafoate [17], terbutaline sulphate [18,19], budesonide [20–22], and flunisolide [20,21]. In general, SCF technologies fall into two broad groups: a supercritical solvent process and a supercritical antisolvent process, according to the role of the SCF and use of a second solvent. In the former group, the solute is directly solubilized in the compressed CO₂. In the latter case, generally referred to as supercritical anti-solvent (SAS) processes, the solute is dissolved in a second solvent (usually an organic solvent) and the solution is contacted with the compressed CO₂ which acts as an antisolvent causes powder formulation by solute precipitation. Many pharmaceutical substances have been micronized by the SAS process because of the low solubility of pharmaceutical drugs in supercritical CO₂. Various SAS processes have been described in the literature, including: an aerosol solvent extraction system (ASES), precipitation with a compressed antisolvent (PCA) or solution enhancement dispersion by supercritical fluids (SEDS). The ASES/PCA process uses a single nozzle and the SEDS process uses a co-axial nozzle with a mixing chamber that increases mass transfer rate between supercritical CO₂ and drug solution. Although nozzle design in SEDS process is complicated and expensive, this process is

useful for micronizing new polymorphs of pharmaceutical drugs, especially water soluble drugs [17,18,21].

In the present study, we use the ASES [23–25], one of the supercritical antisolvent methods, to ascertain the feasibility of micronization of ipratropium bromide (IB) for pulmonary delivery. In the ASES process, a solution or dispersion of a drug in an organic solvent is sprayed into a continuous stream of a supercritical fluid (typically CO₂). The solvent, which is miscible with the supercritical CO₂, is extracted at the operating conditions; while the drug, being much less soluble in the supercritical CO₂, is precipitated as micro-particles. IB is a quaternary ammonium anticholinergic bronchodilator administered by inhalation [26]. IB in aerosol form has been shown to have an effect in asthma and chronic obstructive pulmonary disease (COPD) [27], whereas oral doses are not therapeutic. In this study, IB particles precipitated by ASES processing were characterized using scanning electron microscopy (SEM), and fourier transform infrared (FTIR) spectrophotometry in order to examine the aerodynamic particle size, morphology, and possible structural deformations under various operating conditions. In addition, to assess the optimal particle size for deposition in the deep lung area, a mathematical deposition model for inhaled particles in the human respiratory tract is applied to the particles formed.

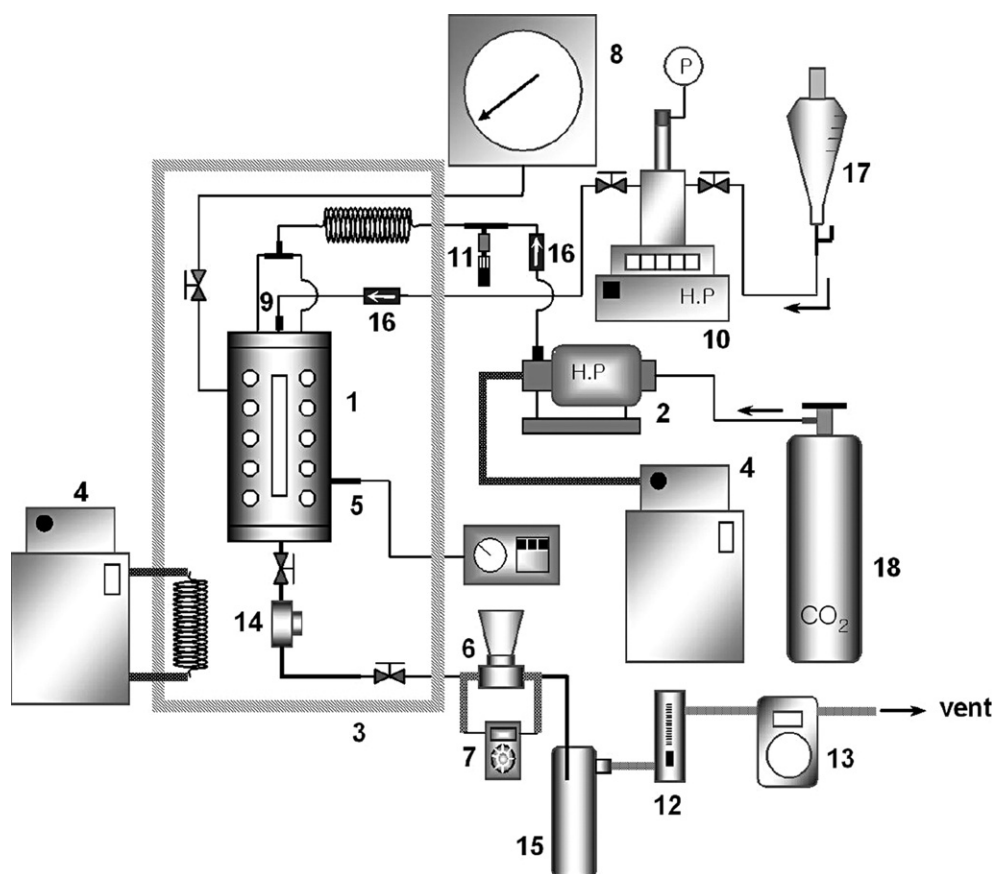


Fig. 1. The experimental apparatus used for ASES process. (1) precipitation vessel, (2) high pressure pump, (3) air bath, (4) refrigerated circulator, (5) thermo couple, (6) back pressure regulator, (7) heating controller, (8) pressure gauge, (9) nozzle (I.D. 254 μm), (10) high pressure pump, (11) metering valve, (12) rotameter, (13) gas meter, (14) metal filter (0.5 μm), (15) separator, (16) check valve, (17) drug solution reservoir, (18) liquid CO₂.

2. Materials and methods

2.1. Materials

Ipratropium bromide (IB, purity >99%) was purchased from Sigma-Aldrich (ST. Louis, MO). Ethanol (EtOH, purity 100%) was purchased from Aaper Alcohol and Chemical Co. (Shelbyville, KY). Dimethylformamide (DMF, purity 99.9%) and Acetone (Ac, purity 99.9%) were purchased from Burdick and Jackson (Muskegon, MI). Carbon dioxide (CO₂) (purity 99.8%) was purchased from Gilmore (South El Monte, CA). All of the chemicals were used as received without further purification.

2.2. ASES apparatus and procedures

The schematic diagram of the ASES apparatus is shown in Fig. 1. The windowed precipitation vessel ((1), i.v. = 100 cm³, i.d. = 3.4 cm) was pressurized with CO₂ using a reciprocating pump ((2), Milton Roy, model Minipump). Operating temperatures were maintained by air heated-bath ((3), Ruska, model 2320) and a heat exchanger connected to an auxiliary thermostatic bath ((4), Haake, model A82). The temperature was measured by a K-type thermocouple ((5), Omega, model TJ36-CASS-18G-12) and digital indicator (Omega, model CN132) with an accuracy of ±0.1 °C. The vessel pressure was controlled by a back-pressure regulator ((6), Tescom, model 26-IN62-24), heated by a heating tape ((7), Barnstead, model BS0051-020) to prevent plugging in the valve due to CO₂ depressurization. The pressure in the vessel is measured using a

dial pressure gauge ((8), Heise, model CMM 55214). After steady pressure, temperature, and CO₂ flow rate were achieved, the solution containing the drug was injected co-current with the CO₂ into the precipitation vessel through a 254 µm internal diameter stainless steel capillary tubing ((9), Supelco, model 56720-U) using a computer controlled syringe pump ((10), ISCO, model 100D). The CO₂ was continuously fed through the vessel at constant flow rate controlled by the fine metering valve ((11), Hoke, model 1315G2Y) and by adjusting the power of the pump. At the end of each experiment, the flow of drug solution was stopped, and fresh CO₂ added to the precipitation vessel to wash and dry the precipitated particles. After washing was complete, a small amount of CO₂ was vented through the nozzle to remove any remaining solution, and then most CO₂ was purged through a back-pressure regulator. The CO₂ flow rate was measured with a rotameter ((12), Matheson, model KIT-0150-AO) and a dry gas meter ((13), Apex, model SK25). The vessel was depressurized, and precipitated particles were collected at the bottom of the vessel where a metal filter ((14), Swagelok, model SS-4TF-05) prevents venting of the precipitated particles. A range of operating pressures (140–200 bar) and temperatures (40–60 °C) was applied to produce micronized drug particles using the ASES process.

2.3. Particle characterization

2.3.1. Scanning electron microscopy (SEM)

Images of the IB particles were taken using a SEM (Cambridge, model 360). Drug samples were fixed by double-

Table 1
Experimental conditions and resulting particle morphology

Experiment number	Solvent (v:v)	Pressure (bar)	Temperature (°C)	Density ^a (CO ₂) (g/cm ³)	Solution conc. (mg/ml)	Solution flow rate (ml/min)	AMAD ^b (µm)	Notes
1	EtOH	200	50	0.79	10	2	NA ^c	Irregular, flaky
2	EtOH/Ac (34:66)	140	60	0.56	15	1	NA	Irregular
3	EtOH/Ac (34:66)	180	50	0.76	15	1	NA	Irregular
4	EtOH/Ac (34:66)	200	40	0.84	10	1	5.04	Slightly spherical, some agglomeration
5	EtOH/Ac (34:66)	200	50	0.79	10	2	6.54	Slightly spherical, some agglomeration
6	EtOH/Ac (34:66)	200	50	0.79	15	1	6.74	Slightly spherical, some agglomeration
7	EtOH/Ac (34:66)	200	50	0.79	15	2	NA	Irregular
8	EtOH/Ac (34:66)	200	50	0.79	20	1	NA	Irregular
9	EtOH/Ac (34:66)	200	60	0.73	15	1	NA	Irregular, some agglomeration
10	DMF	200	40	0.84	10	2	1.86	Elliptical, discrete, uniform
11	DMF	200	40	0.84	20	2	NA	Irregular
12	DMF	200	50	0.79	10	2	1.95	Elliptical, discrete, uniform
13	DMF	200	50	0.79	10	3.5	NA	Irregular
14	DMF	160	50	0.72	10	2	4.48	Elliptical, discrete

^a S. Angus et al. [39].

^b AMAD: arithmetic mean aerodynamic diameter which was calculated from SEM pictures.

^c Not available.

sided conductive adhesive tape (Ted pella) on the aluminum stub and covered with gold under an argon atmosphere (40 Pa) at 50 μA for 60 s using a sputter coater (Ernest F. Fullam, model EMS-76M). Particle size distribution and the mass median particle diameter were determined on the basis of mean projected area of about 500 particle images using an image analysis software (Image J, National Institutes of Health).

2.3.2. Aerodynamic particle size analysis

The aerodynamic diameter of a particle, d_a , is defined as the diameter of an equivalent spherical particle with a density of 1 g/cm^3 that has the same settling velocity as the particle of interest. It is the key particle property for characterizing respiratory deposition [28]. The aerodynamic diameter is given by

$$d_a = d_e \left(\frac{\rho_p}{\rho_0 \chi} \right)^{1/2} = d_p \left(\frac{\rho_p}{\rho_0} \right)^{1/2} \quad (1)$$

where ρ_p = particle density, ρ_0 = standard particle density (1 g/cm^3), d_e = equivalent volume diameter, d_p = particle diameter, χ = dynamic shape factor. The true density of IB (ρ_p) was measured by a multipycnometer (Quantachrome, model MVP-1) with a 4.5 cm^3 sample cell. Five measurements were performed for every sample to obtain mean values. The mean and standard deviation of measured true density of IB particle was $1.326 \pm 0.081 \text{ g}/\text{cm}^3$. We used $\chi=1$ in calculating the aerodynamic diameters for two reasons: first, the particles are somewhat irregular in shape, second, it is known that except for highly nonspherical particles, the errors introduced in assuming $\chi=1$ are not significant.

Inhaled aerosols are typically described by the logarithm of the size distributions rather than the size itself because most aerosols exhibit a skewed distribution function with a long tail. Two important statistical properties of inhaled drug particles are the mass median aerodynamic diameter (MMAD) and the geometric standard deviation (GSD). The SEM images analysis yields the number based size distribution from which the GSD (σ_g) can be obtained as:

$$\sigma_g = \sqrt{\frac{d_{84\%}}{d_{16\%}}} \quad (2)$$

where $d_{84\%}$ = the size associated with a cumulative count of 84% $d_{16\%}$ = the size associated with a cumulative count of 16%. The number based particle size distribution is then converted to a mass based particle size distribution using

$$\frac{dM}{M_T \text{dlog} d_a} = \frac{dN}{N_T \text{dlog} d_a} \left(\frac{\pi}{6} d_a^3 \rho_p \right) \quad (3)$$

where M_T = total mass of measured particles, N_T = total number of measured particles, $dM/M_T \text{dlog} d_a$ and $dN/N_T \text{dlog} d_a$ are the normalized mass and number concentration, respectively. The MMAD is then obtained from the mass based particle size distribution.

2.3.3. Fourier transform infrared (FTIR) spectrophotometry

FTIR spectrophotometry analysis was conducted with a Genesis II (Mattson, model 960M0000) in the range 600–4000 cm^{-1} , using a resolution of 2 cm^{-1} and 100 scans. Control of the instrument, as well as collection and primary analysis of

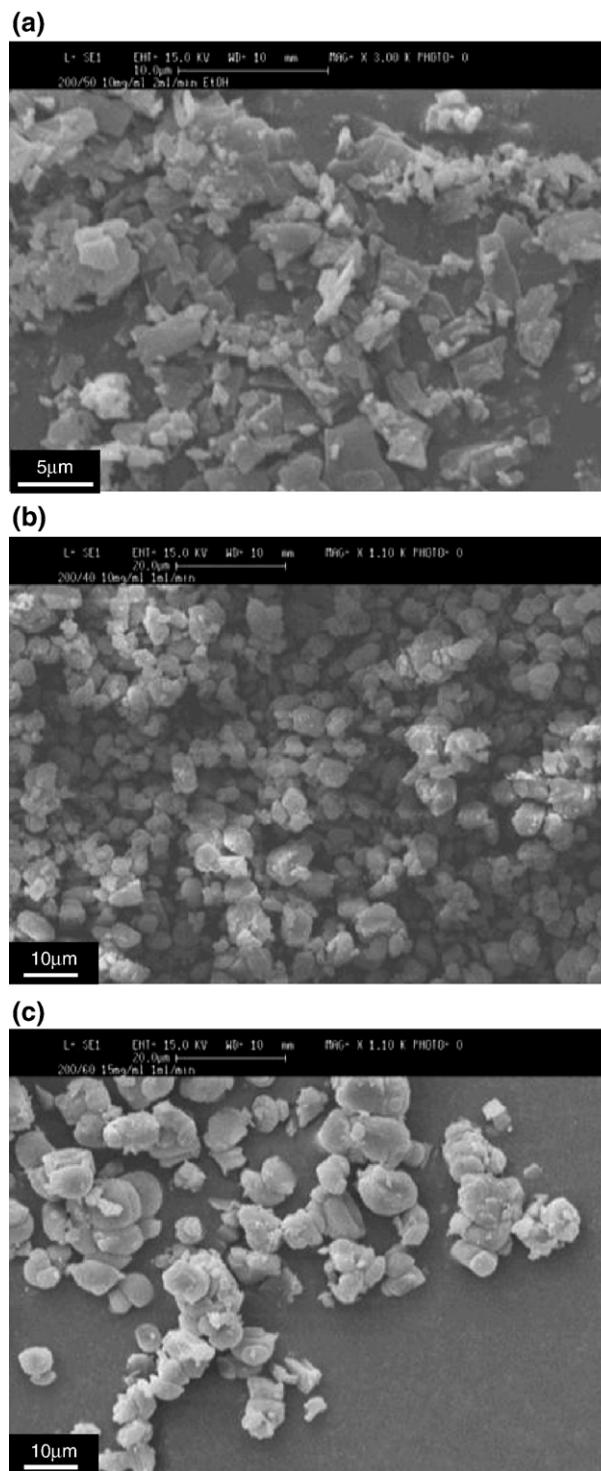


Fig. 2. SEM pictures of IB particles: (a) precipitated from EtOH at 50 °C, 200 bar, 10 mg/ml, and 2 ml/min, (b) EtOH/Ac at 40 °C, 200 bar, 10 mg/ml, and 1 ml/min, (c) EtOH/Ac at 60 °C, 200 bar, 15 mg/ml, and 1 ml/min.

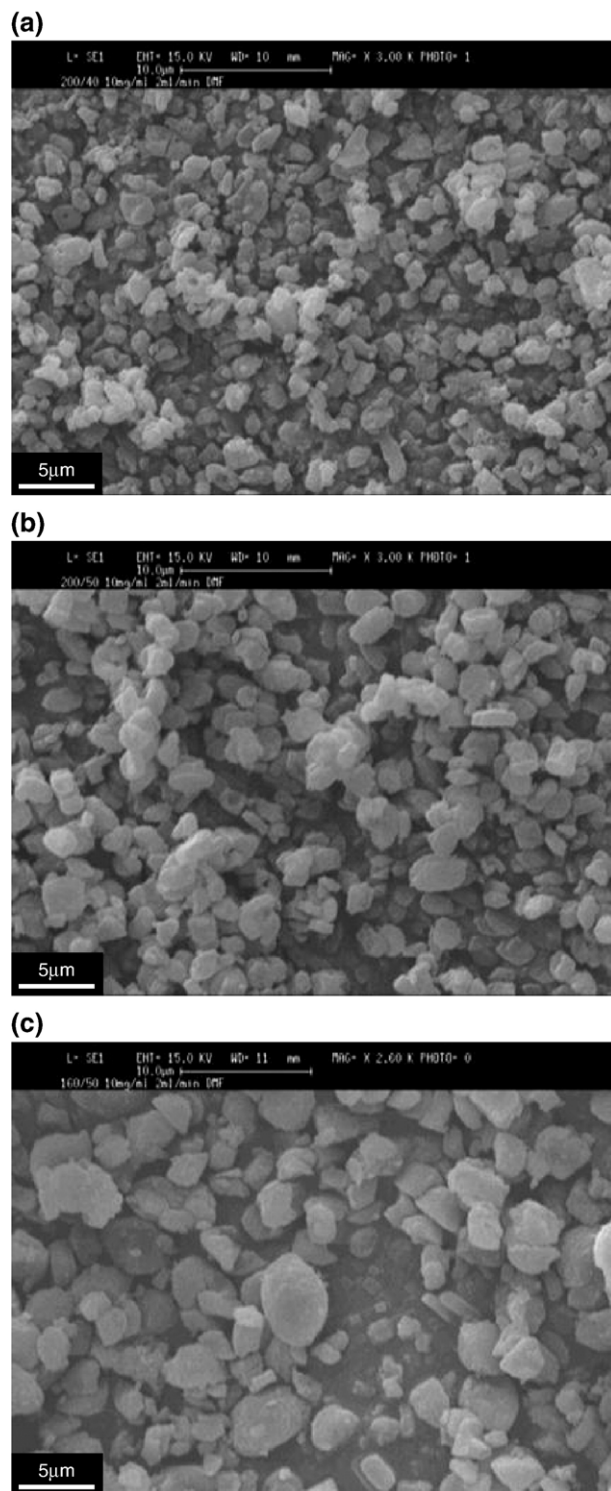


Fig. 3. SEM pictures of IB particles: (a) precipitated from DMF at 40 °C, 200 bar, 10 mg/ml, and 2 ml/min, (b) 50 °C, 200 bar, 10 mg/ml, and 2 ml/min, (c) 50 °C, 160 bar, 10 mg/ml, and 2 ml/min.

data, was accomplished using WinFirst software (Mattson). Samples were diluted with KBr mixing powder at 1% and pressed with a KBr Die Kit and a hydraulic press (DAKE, model 44–226) to obtain self-supporting disks.

2.3.4. Mathematical deposition model for inhaled particles

The early deposition models presented by Findeisen [29] and Landahl [30] assumed relatively simple lung morphologies, simple deposition mechanisms of inhaled particles and limited physical characteristics of inhaled particles. More recently, several models have been developed [31–33] which can calculate deposition fractions for extrathoracic, tracheobronchial and pulmonary regions with respect to different breathing patterns, age and sex. Although the alveolar region is still idealized, these models are more realistic than the early deposition models by improving the modeling of the respiratory airways, the fluid dynamics, particle transport and physiological processes. In the present work, we used the multiple-path model of particle deposition (MPPD v1.0, Chemical Industry Institute of Toxicology) based on morphometric model generated from extensive actual lung structures of humans. Asgharian et al. [33] showed the multiple-path model was able to predict more accurate lobar deposition fractions when compared to a typical-path symmetric lung model [34]. The particle properties determined in this work are used to estimate the deposition fractions by applying the MMPD.

3. Results and discussion

3.1. Particle morphology

It is generally known that particles produced by ASES process tend to be more spherical in shape and less crystalline than those produced by SEDS process [20–22]. Ipratropium bromide (IB) freely dissolves in water and lower alcohols, but is insoluble in lipophilic solvents such as ether, chloroform and fluorocarbons. In general, good solvents produce larger particles, because supersaturation is reached too slowly and particle growth is favored [35]. In supercritical antisolvent process, the particle size, morphology and crystallinity are dependent on a number of factors such as the solution flow rate, drug concentration, CO₂ flow rate, nozzle diameter, operating pressure, and temperature. Because of the large number of variables, the effects of varying a single parameter do not follow well-defined consistent pattern [10]. For this study, the CO₂ flow rate was fixed at 1.5 SLPM (standard liter per minute). Other experimental conditions used in this work are listed in Table 1.

Limited variations in temperature, pressure, and solution feed rates were made in order to search the optimum combinations of operating conditions that would result in the

Table 2
Particle size distribution of IB precipitated from EtOH/Ac and DMF

Sample ^a	D ₁₀ (μm)	D ₅₀ (μm) ^b	D ₉₀ (μm)	GSD ^c
Experiment 4	4.51	6.02	7.57	1.23
Experiment 5	5.42	7.39	9.38	1.23
Experiment 10	1.62	2.22	2.83	1.31
Experiment 12	1.91	2.68	3.87	1.32
Experiment 14	3.29	4.83	7.34	1.38

^a For experimental conditions, see Table 1.

^b D₅₀ indicates mass median aerodynamic diameter (MMAD).

^c GSD: geometric standard deviation.

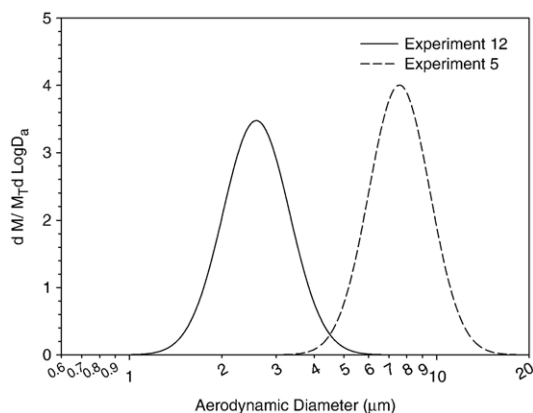


Fig. 4. Normalized PSDs from SEM images of IB particles precipitated from DMF and EtOH/Ac at the same operating conditions.

formation of drug particles suitable for pulmonary delivery. Observations summarized in Table 1 indicate that high solution flow rate and/or high solution concentration tend to result in larger and irregular particles, probably due to agglomeration of smaller particles. Increasing the operating temperature tends to increase the particle size (experiments 4, 6 and 9; experiments 10 and 12), as well as making the particles less uniform in size (Fig. 2b and c; Fig. 3a and b). This is probably because as temperature increases, IB becomes more soluble in EtOH/Ac or DMF while CO₂ becomes less soluble, hence reducing the level of supersaturation and slowing down the particle formation process. Similar observations were noted in other published studies [36–38]. The effect of changing the operating pressure is primarily to change the density of the supercritical CO₂. At lower pressure, the CO₂ density is lower, hence diminishing its compatibility with (or solubility in) the organic solvent. Mass transfer rates are reduced, resulting in slower nucleation rates and larger particles. (Table 1, experiments 2, 3, and 4; experiments 12 and 14). Similar behavior is observed in other studies [37,38].

The parameter that had the greatest effect on particle size is the choice of solvent since it directly affects the IB solubility (hence the extent of supersaturation) as well as the drying rate of the wet particles through its effect on CO₂ solubility and mass transfer. Three solvent systems were studied: pure EtOH, EtOH/

Ac and DMF. Table 1 indicates that the solvent choice results in very different particle size and size distribution under otherwise identical operating conditions. The initial choice of EtOH as solvent resulted in large (4–15 μm) and very irregular, flaky particles, clearly unsuitable for inhalation therapy (Fig. 2a). This is most likely due to the low level of supersaturation (i.e. EtOH is too good a solvent for IB). In order to increase the supersaturation level, we mixed EtOH with Ac which is a poor solvent for IB. Addition of 66 vol.% Ac to EtOH induces an increase in the supersaturation level and hence an increase in the nucleation rate. SEM pictures of ASES precipitated IB from EtOH/Ac at different conditions are shown in Fig. 2b and c. Compare to pure EtOH solvent (Fig. 2a), the particle size and shape are significantly improved. The particles are more spherical, however, they are still too large for inhalation therapy. As mentioned above, the mass median aerodynamic diameter (MMAD) of drug particle should be in the range from 1 to 5 μm for deep lung deposition. Indeed, all IB particles precipitated from EtOH and EtOH/Ac were too large as shown in Fig. 2 and Table 1. Thus, another solvent, DMF, was chosen to reduce the particle size. The first selection of operating conditions was based on experiment 4, because it showed the best micronization result using EtOH/Ac. SEM images of IB particles formed from DMF are shown in Fig. 3. We see that compared to EtOH/Ac, IB particles formed from DMF at the condition studied were more regular in shape, slightly elliptical, not agglomerated, and smaller in size (2–5 μm). These particles are suitable in size for pulmonary delivery.

The sensitive dependence of particle morphology on solvent choice was also observed in ASES processing of other drugs such as salbutamol particles [16]. When suitable solvents are used, particles of other asthma or COPD drugs such as budesonide [20,22] and terbutaline [19] produced by SCF processing are more or less spherical; the average particle size can be optimized by varying the operating conditions such as pressure, temperature, solution flow rate, etc.

3.2. Particle size distribution

SEM images visually show the qualitative information of particle size and distribution. Image analysis software is used to

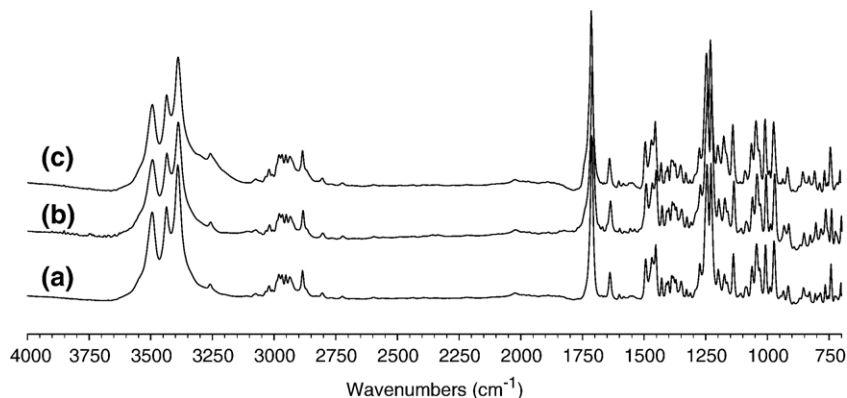


Fig. 5. FT-IR spectra of untreated and ASES precipitated IB: (a) untreated IB, (b) precipitated from DMF at 40 °C, 200 bar, 10 mg/ml, and 2 ml/min, (c) EtOH/Ac at 60 °C, 140 bar, 15 mg/ml, and 1 ml/min.

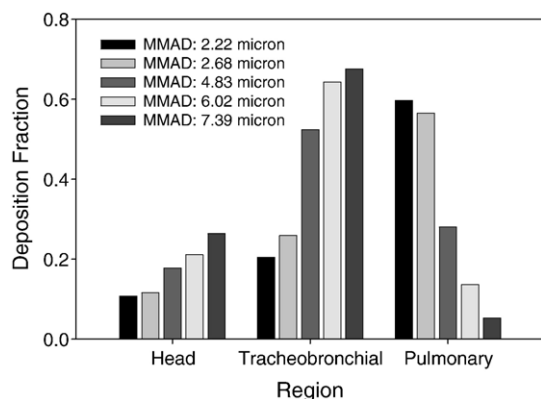


Fig. 6. Deposition fraction of IB particles precipitated by the ASES process as the human lung and extrathoracic region according to the program MMPD.

further quantify particle size and particle size distribution (PSD). The geometric standard deviations are calculated using Eq. (2) and shown in Table 2. The number based PSDs are then converted to mass based PSDs using Eq. (3), from which three mass based diameters D_{10} , D_{50} , D_{90} are shown in Table 2. D_{50} is the aerodynamic diameter where 50% of the mass is distributed among particles with $D > D_{50}$, hence D_{50} is also the MMAD.

Table 2 quantitatively shows that a temperature increase from 40 °C to 50 °C increased the MMAD for IB in EtOH/Ac from 6.02 to 7.39 μm . The MMAD increase in DMF is from 2.22 to 2.68 μm . Fig. 4 shown a comparison of the PSD for particles produced in EtOH/Ac and in DMF at the same conditions. It is clear that changing the solvent from EtOH/Ac to DMF significantly reduces the particle size.

3.3. FTIR data analysis

IB structure before and after ASES processing is studied using FTIR spectroscopy. Spectra of untreated and IB precipitated from DMF, EtOH and EtOH/Ac are shown in Fig. 5. Peak-by-peak correlation [40] was performed for untreated IB and ASES precipitated IB. No significant differences are observed. This is perhaps not surprising because IB is a relatively low molecular weight compound.

3.4. Estimation of regional deposition in human lung

To compare the inhalation deposition performance of the IB particles produced by the ASES process under various operating conditions, we used the multiple-path model of particle deposition (MPPD v1.0, Chemical Industry Institute of Toxicology) to generate the deposition fractions. The model calculates the mass fraction deposited in various parts of the respiratory tract. We assumed an average inspiratory flow rate of 50 L/min, a tidal volume of 700 cm^3 , breathing frequency of 5 breaths/min and a breath pause of 10 s. In addition, particles were assumed to enter the lung via mouth so that head deposition takes place only in the mouth cavity. These conditions are equivalent to those used in experimental studies of Zane et al. [41].

Using the particles size and distribution data reported in Section 3.2, the deposition fraction for the IB particles produced using the ASES process for the experiments listed in Table 2 where the MMAD ranges from 2.22 to 7.39 μm were calculated using the MMPD. The results are shown in Fig. 6. The three samples with large sizes show the largest deposition fraction in the tracheobronchial region. The two samples with the lowest MMAD (2.22 and 2.68 μm) show almost identical deposition fractions, with high deposition fraction in the pulmonary region. This is consistent with the *in vivo* deposition studies reported by Zane et al. [41] who showed that optimal IB particles size for pulmonary delivery in treating asthmatic patients was about 2.8 μm .

4. Conclusions

The ASES process was used to ascertain the feasibility of micronization of IB within the respirable size range. The effect of solvent type, IB concentration, solution flow rate, temperature and pressure were studied. It was found that particle size and morphology could be controlled by varying process parameters. The solvent choice has a large influence on particle morphology and size distribution. The use of EtOH/Ac mixed solvent gives better results with regard to the particle size and shape than pure EtOH. Among the solvents studied in this work, the best ASES processing solvent for IB is DMF. The particles formed from DMF solvent are more regular in shape and showed much less agglomeration. Particle size of 2–3 μm can be achieved which are suitable for use in inhalation therapy. FTIR analysis showed that IB structure was not affected by the ASES process. The deposition fractions of the particles produced in this study were simulated using the recently developed deposition model (MPPD). It was found that IB particles with MMAD of 2.22 and 2.68 μm formed from DMF were within the optimal size range where most of the particles deposit in the pulmonary region. The ASES process is a versatile method for the micronization of IB and other drugs for pulmonary delivery because several operating conditions (such as pressure, temperature, solvent choice, etc) can be manipulated to achieve optimum particle characteristics.

Acknowledgements

The authors acknowledge the use of MPPD V1.0 program from Chemical Industry Institute of Toxicology (Research Triangle Park, NC). A USC WISE grant is gratefully acknowledged.

References

- [1] R.J. Malcolmson, J.K. Embleton, Dry powder formulations for pulmonary delivery, *Pharm. Sci. Technol. Today (PSTT)* 1 (1998) 394–398.
- [2] M.P. Timsina, G.P. Martin, C. Marriott, D. Ganderton, M. Yianneskis, Drug delivery to the respiratory tract using dry powder inhalers, *Int. J. Pharm.* 101 (1994) 1–13.
- [3] R.U. Agu, M.I. Ugwoke, M. Armand, R. Kinget, N. Verbeke, The lung as a route for systemic delivery of therapeutic proteins and peptides, *Respir. Res.* 2 (2001) 198–209.
- [4] S.J. Smith, J.A. Bernstein, Therapeutic uses of lung aerosols, in: A.J. Hickey (Ed.), *Inhalation Aerosols: Physical And Biologic Basis for Therapy*, Marcel Dekker, Inc., New York, 1996, pp. 233–269.

- [5] L.S. Tu, F. Dehghani, N.R. Foster, Micronisation and microencapsulation of pharmaceuticals using a carbon dioxide antisolvent, *Powder Technol.* 126 (2002) 134–149.
- [6] A.J. Hickey, C.A. Dunbar, A new millennium for inhaler technology, *Pharm. Technol.* 21 (1997) 116–125.
- [7] B.Y. Shekunov, Production of powder for respiratory drug delivery, in: P. York, U.B. Kompella, B.Y. Shekunov (Eds.), *Supercritical Fluid Technology for Drug Product Development*, Marcel Dekker, Inc., New York, 2004, pp. 247–282.
- [8] B. Subramaniam, R.A. Rajewski, K. Snavelly, Pharmaceutical processing with supercritical carbon dioxide, *J. Pharm. Sci.* 86 (1997) 885–890.
- [9] E. Reverchon, G.D. Porta, Production of antibiotic micro- and nanoparticles by supercritical antisolvent precipitation, *Powder Technol.* 106 (1999) 23–29.
- [10] E. Reverchon, Supercritical antisolvent precipitation of micro- and nanoparticles, *J. Supercrit. Fluids* 15 (1999) 1–21.
- [11] N.R. Foster, R. Mammucari, F. Dehghani, A. Barrett, K. Bezanhtak, E. Coen, G. Combes, L. Meure, A. Ng, H.L. Regtop, A. Tandy, Processing pharmaceutical compounds using dense gas technology, *Ind. Eng. Chem. Res.* 42 (2003) 6476–6493.
- [12] F. Dehghani, N.R. Foster, Dense gas anti-solvent processes for pharmaceutical formulation, *Curr. Opin. Solid State Mater. Sci.* 7 (2003) 363–369.
- [13] J. Fages, H. Lochard, J.-J. Letourneau, M. Sauceau, E. Rodier, Particle generation for pharmaceutical applications using supercritical fluid technology, *Powder Technol.* 141 (2004) 219–226.
- [14] E. Reverchon, A. Spada, Erythromycin micro-particles produced by supercritical fluid atomization, *Powder Technol.* 141 (2004) 100–108.
- [15] S. Jaamo, M. Rantakyla, O. Aaltonen, Particle tailoring with supercritical fluids: production of amorphous pharmaceutical particles, *Proceedings of the 4th International Symposium on Supercritical Fluids*, Sendai, Japan, May 11–14 1997.
- [16] E. Reverchon, G.D. Porta, P. Pallado, Supercritical antisolvent precipitation of salbutamol microparticles, *Powder Technol.* 114 (2001) 17–22.
- [17] B.Y. Shekunov, J.C. Feeley, A.H.L. Chow, H.H.Y. Tong, P. York, Aerosolisation behaviour of micronised and supercritically-processed powders, *J. Aerosol Sci.* 34 (2003) 553–568.
- [18] M. Rehman, B.Y. Shekunov, P. York, D. Lechuga-Ballesteros, D.P. Miller, T. Tan, P. Colthorpe, Optimisation of powders for pulmonary delivery using supercritical fluid technology, *Eur. J. Pharm. Sci.* 22 (2004) 1–17.
- [19] E. Reverchon, G.D. Porta, Terbutaline microparticles suitable for aerosol delivery produced by supercritical assisted atomization, *Int. J. Pharm.* 258 (2003) 1–9.
- [20] H. Steckel, J. Thies, B.W. Müller, Micronizing of steroids for pulmonary delivery by supercritical carbon dioxide, *Int. J. Pharm.* 152 (1997) 99–110.
- [21] S.P. Velaga, R. Berger, J. Carlfors, Supercritical fluids crystallization of budesonide and flunisolide, *Pharm. Res.* 19 (2002) 1564–1571.
- [22] H. Steckel, L. Pichert, B.W. Müller, Influence of process parameters in the ASES process on particle properties of budesonide for pulmonary delivery, *Eur. J. Pharm. Biopharm.* 57 (2004) 507–512.
- [23] J. Bleich, B.W. Müller, W. Waßmus, Aerosol solvent extraction system — a new microparticle production technique, *Int. J. Pharm.* 97 (1993) 111–117.
- [24] J. Bleich, P. Kleinebudde, B.W. Müller, Influence of gas density and pressure on microparticles produced with the ASES process, *Int. J. Pharm.* 106 (1994) 77–84.
- [25] J. Bleich, B.W. Müller, Production of drug loaded microparticles by the use of supercritical gases with the Aerosol Solvent Extraction System (ASES) process, *J. Microencapsul.* 13 (1996) 131–139.
- [26] G.E. Pakes, R.N. Brogden, R.C. Heel, T.M. Speight, G.S. Avery, Ipratropium bromide: a review of its pharmacological properties and therapeutic efficacy in asthma and chronic bronchitis, *Drugs* 20 (1980) 237–266.
- [27] T.J. Hogan, R. Geddes, E.R. Gonzalez, An economic assessment of inhaled formoterol dry powder versus ipratropium bromide pressurized metered dose inhaler in the treatment of chronic obstructive pulmonary disease, *Clin. Ther.* 25 (2003) 285–297.
- [28] W.C. Hinds, *Aerosol technology-properties, behavior, and measurement of airborne particles*, 2nd ed., John Wiley & Sons, New York, 1999, pp. 42–110.
- [29] W. Findeisen, Über das Absetzen Kleiner, in der Luft suspendierter Teilchen in der menschlichen Lunge bei der Atmung, *Pflügers Arch. D. Gesamte Physiol.* 236 (1935) 367–379.
- [30] H.D. Landahl, On the removal of air-borne droplets by human respiratory tract. I. The lung, *Bull. Math. Biophys.* 12 (1950) 43–56.
- [31] R.F. Phalen, R.G. Cuddihy, G.L. Fisher, O.R. Moss, R.B. Schlesinger, D.L. Swift, H.C. Yeh, Main features of the proposed NCRP respiratory tract model, *Rad. Prot. Dos.* 38 (1991) 179–184.
- [32] W.J. Bair, Overview of ICRP respiratory tract model, *Rad. Prot. Dos.* 38 (1991) 147–152.
- [33] B. Asgharian, W. Hofmann, R. Bergmann, Particle deposition in a multiple-path model of the human lung, *Aerosol Sci. Technol.* 34 (2001) 332–339.
- [34] H.-C. Yeh, G.M. Schum, M.T. Duggan, Anatomic models of the traceobronchial and pulmonary regions of the rat, *Anat. Rec.* 195 (1979) 483–492.
- [35] O. Boutin, E. Badens, E. Carretier, G. Charbit, Co-precipitation of a herbicide and biodegradable materials by the supercritical anti-solvent technique, *J. Supercrit. Fluids* 31 (2004) 89–99.
- [36] B. Warwick, F. Dehghani, N.R. Foster, J.R. Biffin, H.L. Regtop, Micronization of copper indomethacin using gas antisolvent processes, *Ind. Eng. Chem. Res.* 41 (2002) 1993–2004.
- [37] J.O. Werling, P.G. Debenedetti, Numerical modeling of mass transfer in the supercritical antisolvent process: miscible conditions, *J. Supercrit. Fluids* 18 (2000) 11–24.
- [38] A. Martin, M.J. Cocero, Numerical modeling of jet hydrodynamics, mass transfer, and crystallization kinetics in the supercritical antisolvent (SAS) process, *J. Supercrit. Fluids* 32 (2004) 203–219.
- [39] S. Angus, B. Armstrong, K.M. de Reuck, *International Thermodynamic Tables of the Fluid State Carbon Dioxide*, 1st ed., Pergamon Press, New York, 1976, p. 338.
- [40] R.M. Silverstein, G.C. Bassler, T.C. Morrill, *Spectrometric Identification of Organic Compounds*, 5th ed., John Wiley & Sons, Inc., New York, 1991, pp. 91–164.
- [41] P. Zanen, L.T. Go, J.-W.J. Lammers, The optimal particle size for parasympatholytic aerosols in mild asthmatics, *Int. J. Pharm.* 114 (1995) 111–115.